Spectrum- and Energy-Efficient OFDM Based on Simultaneous Multi-Channel Reconstruction

Linglong Dai, Jintao Wang, Zhaocheng Wang, Paschalis Tsiaflakis, and Marc Moonen

***Abstract*—Time domain synchronous OFDM (TDS-OFDM) has a higher spectrum and energy efficiency than standard cyclic prefix OFDM (CP-OFDM) by replacing the unknown CP with a known pseudorandom noise (PN) sequence. However, due to mutual interference between the PN sequence and the OFDM data block, TDS-OFDM cannot support high-order modulation schemes such as 256QAM in realistic static channels with large delay spread or high-definition television (HDTV) delivery in fast fading channels. To solve these problems, we propose the idea of using multiple inter-block-interference (IBI)-free regions of small size to realize simultaneous multi-channel reconstruction under the framework of structured compressive sensing (SCS). This is enabled by jointly exploiting the sparsity of wireless channels as well as the characteristic that path delays vary much slower than path gains. In this way, the mutually conditional time-domain channel estimation and frequency-domain data demodulation in TDS-OFDM can be decoupled without the use of iterative interference removal. The Cramér-Rao lower bound (CRLB) of the proposed estimation scheme is also derived. Moreover, the guard interval amplitude in TDS-OFDM can be reduced to improve the energy efficiency, which is infeasible for CP-OFDM. Simulation results demonstrate that the proposed SCS-aided TDS-OFDM scheme has a higher spectrum and energy efficiency than CP-OFDM by more than 10% and 20% respectively in typical applications.**

***Index Terms*—Spectrum and energy efficiency; TDS-OFDM; CP-OFDM; Interference cancellation; Channel estimation.**

I. Introduction

SPECTRUM and energy efficiency are of great importance for present and future wireless communication systems [1]. OFDM has already been extensively adopted by numerous wireless communication systems like DVB-T, WiMAX, LTE, WiFi, etc, and it is also widely recognized as a prominent modulation technique for future wireless communication systems [2]. Thus, developing spectrum- and energy-efficient OFDM scheme is essential to achieve high transmission efficiency and low energy consumption.

There are three basic types of OFDM: cyclic prefix OFDM (CP-OFDM) [2], zero padding OFDM (ZP-OFDM) [3], and time domain synchronous OFDM (TDS-OFDM) [4]. The popular CP-OFDM utilizes a CP as a guard interval to alleviate inter-block-interference (IBI) in multipath channels [5]. The CP is replaced by a ZP in ZP-OFDM to tackle the channel transmission zeros problem [3]. Unlike CP-OFDM or ZP-OFDM, TDS-OFDM adopts a known pseudorandom noise (PN) sequence as a guard interval as well as a training sequence (TS) for synchronization and channel estimation. Consequently, it does not require any frequency-domain pilots as usually used in CP-OFDM and ZP-OFDM, leading to a higher spectrum and energy efficiency [4]. TDS-OFDM[1] is the key technology of Chinese digital television terrestrial broadcasting (DTTB) standard called digital terrestrial multimedia/television broadcasting (DTMB) [7], which has been successfully deployed in China, Laos, Cuba, etc. In December 2011, DTMB was officially approved by ITU as an international DTTB standard [8].

One direct way to increase the OFDM system spectrum efficiency is to use higher order of modulations. For example, both the recently announced next-generation DTTB standard DVB-T2 [9] and the emerging WiFi standard IEEE 802.11ac [10] based on CP-OFDM have extended the modulation order from 64QAM to 256QAM to achieve a 30% higher spectrum efficiency. For TDS-OFDM systems, the TS (PN sequence[2]) and the OFDM data block within every TDS-OFDM symbol will introduce mutual interference to each other. Thus, an iterative interference cancellation has to be implemented to achieve reliable time-domain channel estimation and frequency-domain data demodulation in an iterative manner [11]. Due to this mutual interference, TDS-OFDM currently cannot support very high-order constellation scheme like 256QAM in multipath channels with large delay spread (currently, the highest order of constellations that can be supported by TDS-OFDM is 64QAM [7]). This is because 256QAM is very sensitive to the residual interference, which is hard to be completely removed in TDS-OFDM. Meanwhile,

Manuscript received February 9, 2013; revised June 6 and August 26, 2013. Part of this work has been presented in the IEEE International Conference on Communications (ICC), Budapest, Hungary, June, 2013.

L. Dai, J. Wang, and Z. Wang are with the Department of Electronic Engineering, Tsinghua University, Beijing 100084, P. R. China (e-mails: {daill, wangjintao, zcwang}@tsinghua.edu.cn). Their work was supported by National Key Basic Research Program of China (No. 2013CB329203), National Natural Science Foundation of China (Grant Nos. 61271266, 61201185), and Tsinghua University-KU Leuven Bilateral Scientific Cooperation Foundation (Grant No. BIL11/21T).

P. Tsiaflakis and M. Moonen are with the Electrical Engineering Department (ESAT-SCD), KU Leuven, Belgium (e-mails: {paschalis.tsiaflakis, marc.moonen}@esat.kuleuven.be). P. Tsiaflakis is a postdoctoral fellow funded by the Research Foundation–Flanders (FWO). Their work was supported by Belgian Programme on Interuniversity Attraction Poles initiated by the Belgian Federal Science Policy Office: IUAP P7/'Dynamical systems, control and optimization' (DYSCO), 2012-2017, IUAP P7/23 BESTCOM, 2012-2017, and Concerted Research Action GOA-MaNet.

[1]In the literature, TDS-OFDM is essentially similar to known symbol padding OFDM (KSP-OFDM) and pseudo random postfix OFDM (PRP-OFDM), wherein they all use a known TS instead of a CP as the guard interval [6].

[2]Without loss of generality, the term "TS" usually represents "PN sequence" used by TDS-OFDM in this paper.

TDS-OFDM also cannot support high-definition television (HDTV) delivery in fast fading channels. This is due to the obvious performance degradation of TDS-OFDM when the channel is varying fast, whereby inaccurate data demodulation results in a deteriorated channel estimation, which in turn degrades the data demodulation performance further.

Extensive efforts have been endeavored to solve the interference problem of TDS-OFDM [12]–[20]. Generally, they can be divided into two categories. The first one tries to enhance the performance of the classical iterative interference cancellation algorithm without changing the basic signal structure of TDS-OFDM [12]–[16]. However, only slight improvements can be obtained. The other category relies on modification of the TDS-OFDM signal structure in a preferred way for easier interference cancellation [17]–[20]. For example, the unique word OFDM (UW-OFDM) scheme [17] uses redundant frequecy-domain pilots scattered within the OFDM data block to generate the time-domain TS so that the interference imposed on the OFDM data block can be naturally avoided, but it does not remove the interference from the OFDM data block to the TS. Another simple yet efficient solution is the dual PN padding OFDM (DPN-OFDM) scheme [18], [19], whereby two repeated PN sequences are used in every TDS-OFDM symbol to avoid the interference from the OFDM data block to the second PN sequence. However, the extra PN sequence decreases the spectrum efficiency. Recently, we have proposed the time-frequency training OFDM (TFT-OFDM) scheme [20] by adding a small amount of frequency-domain pilots in TDS-OFDM to avoid the conventional iterative interference cancellation, but performance degradation will be introduced when the interference is severe in multipath channels with large delay spread or fast variation.

In this paper, to provide a more spectrum- and energy-efficient alternative to the standard CP-OFDM scheme, we utilize the newly emerging theory of structured compressive sensing (SCS) [21] to address the problems of conventional TDS-OFDM without changing its signal structure. Specifically, the contributions of this paper are as follows:

1) Wireless channel properties including channel sparsity and the fact that path delays vary much slower than path gains, which are usually not considered in conventional OFDM schemes, are exploited in the proposed SCS-aided TDS-OFDM scheme. Unlike the conventional approach that the interference imposed on the received TS must be removed in TDS-OFDM, we propose the idea of using multiple IBI-free regions of very small size to realize simultaneous multi-channel reconstruction under the framework of SCS. This mechanism requires no change of the basic signal structure of TDS-OFDM, and the mutually conditional time-domain channel estimation and frequency-domain data detection can be decoupled without the use of iterative interference cancellation;
2) Based on the classical sparse signal reconstruction algorithm called simultaneous orthogonal matching pursuit (SOMP) [22] and the joint time-frequency processing feature of TDS-OFDM, we propose the adaptive SOMP (A-SOMP) algorithm, which is adaptive to the channel variation by using the partial channel priori obtained from the contaminated TS in TDS-OFDM. The proposed A-SOMP algorithm has an improved performance and much lower computational complexity than SOMP due to the use of channel priori information;
3) Since the simultaneous multi-channel reconstruction based on A-SOMP can achieve a sufficiently reliable channel estimate, we propose to decrease the amplitude of the guard interval in TDS-OFDM, which is infeasible in classical CP-OFDM, to further improve the energy efficiency of TDS-OFDM. It is shown that the proposed SCS-aided TDS-OFDM scheme has a more than 10% higher spectrum efficiency and a more than 20% higher energy efficiency than CP-OFDM in typical wireless broadcasting applications;
4) We show that the simultaneous multi-channel reconstruction can approach the theoretical Cramér-Rao lower bound (CRLB) as derived in this paper, and by means of simulation results we demonstrate that the proposed SCS-aided TDS-OFDM scheme can support 256QAM in realistic static channels with large delay spread and HDTV delivery in fast fading channels, with a bit error rate (BER) performance close to the ideal channel information case.

The rest of this paper is organized as follows. The system model of the proposed SCS-aided TDS-OFDM scheme is presented in Section II. The simultaneous multi-channel reconstruction method based on A-SOMP is proposed in Section III. Section IV provides the performance analysis of the proposed scheme. In Section V, simulation results are presented to demonstrate the performance of the proposed scheme. Finally, conclusions are drawn in Section VI.

Notation: Boldface letters denote matrices and column vectors; $\mathbf{0}$ denotes the zero matrix of arbitrary size; $\mathbf{F}_N$ denotes the normalized $N \times N$ discrete Fourier transform (DFT) matrix whose $(n+1, k+1)$th entry is $\exp(-j2\pi nk/N)/\sqrt{N}$; $\otimes$ presents the circular correlation; $(\cdot)^T$, $(\cdot)^H$, $(\cdot)^{-1}$, $(\cdot)^\dagger$, and $\|\cdot\|_p$ denote the transpose, conjugate transpose, matrix inversion, Moore-Penrose matrix inversion, and l_p norm operation, respectively; $\mathbf{x}_r$ is generated by restricting the vector $\mathbf{x}$ to its r largest components; $\mathbf{x}|_\Gamma$ denotes the entries of the vector $\mathbf{x}$ in the set Γ; $\mathbf{\Phi}_\Gamma$ denotes the column submatrix comprising the Γ columns of $\mathbf{\Phi}$; $\mathrm{supp}\{\mathbf{\Phi}\}$ is the support of $\mathbf{\Phi}$; Γ^c is the complementary set of Γ; $a_{k,j}$ denotes the (k,j)th entry of the matrix $\mathbf{A}$; Finally, $\mathrm{Tr}\{\cdot\}$ and $\mathrm{E}\{\cdot\}$ are trace and expectation operators, respectively.

II. System Model

In this section, the basic principle and main problems of TDS-OFDM are reviewed first. The sparsity and inter-channel correlation of wireless channels are then discussed, which will be utilized in the proposed SCS-aided TDS-OFDM scheme based on simultaneous multi-channel reconstruction.

A. Basic Principle and Main Problems of TDS-OFDM

TDS-OFDM differs from CP-OFDM and ZP-OFDM by replacing the CP or ZP with a known PN sequence. Besides serving as the guard interval of the subsequent OFDM data

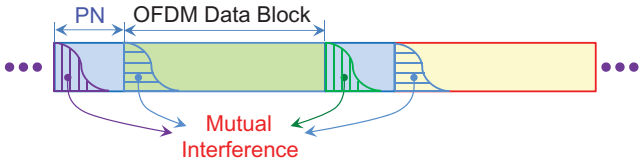

Fig. 1. The mutual interference between the PN sequence and the OFDM data block in multipath channels, which couples the time-domain channel estimation and the frequency-domain data demodulation in TDS-OFDM due to the required iterative interference cancellation.

block, the PN sequence is also reused as the time-domain TS for synchronization and channel estimation. Thus, unlike CP-OFDM or ZP-OFDM, TDS-OFDM requires no frequency-domain pilots, leading to an increased spectrum efficiency by about 10% compared to CP-OFDM [8].

The ith time-domain TDS-OFDM symbol $\mathbf{s}_i = [s_{i,0}, s_{i,1}, \cdots, s_{i,M+N-1}]^T$ comprises the known PN sequence $\mathbf{c}_i = [c_{i,0}, c_{i,1}, \cdots, c_{i,M-1}]^T$ of length M and the OFDM data block $\mathbf{x}_i = [x_{i,0}, x_{i,1}, \cdots, x_{i,N-1}]^T$ of length N, and is denoted as

$$\mathbf{s}_i = \left[\begin{array}{c} \mathbf{c}_i \\ \mathbf{x}_i \end{array}\right]_{(M+N)\times 1} = \left[\begin{array}{c} \mathbf{c}_i \\ \mathbf{F}_N^H \widetilde{\mathbf{x}}_i \end{array}\right]_{(M+N)\times 1}, \quad (1)$$

where $\widetilde{\mathbf{x}}_i = \mathbf{F}_N \mathbf{x}_i$ denotes the frequency-domain data.

As illustrated in Fig. 1, the PN sequence and the OFDM data block introduce mutual interference to each other in multipath channels. The basic principle of TDS-OFDM is that, with perfect channel information, the contribution of the PN sequence can be completely subtracted from the received OFDM data block, and then the received TDS-OFDM symbol is essentially equivalent to a ZP-OFDM symbol, which can be converted to a CP-OFDM symbol by the classical overlap and add (OLA) scheme to realize low-complexity channel equalization [23]. Therefore, accurate channel estimation is essential for TDS-OFDM to achieve a high spectrum and energy efficiency.

However, it is clear from Fig. 1 that a reliable PN-based channel estimation requires a correctly demodulated previous OFDM data block as well as accurate channel information to remove the interference imposed on the received PN sequence. Similarly, a correct data demodulation requires accurate channel information to remove the interference on the OFDM data block caused by the previous PN sequence. That is to say, the coupled channel estimation and data demodulation are mutually conditional due to the mutual interference. Therefore, the classical iterative interference cancellation algorithm has been proposed to refine channel estimation and data demodulation iteratively [11]–[13].

B. Sparsity and Inter-Channel Correlation of Wireless Channels

As discussed before, accurate channel estimation is essential for TDS-OFDM. By taking into account specific properties of wireless channels, one can expect improved channel estimation performance.

For multipath channels, the length-L channel impulse response (CIR) $\mathbf{h}_i = [h_{i,0}, h_{i,1}, \cdots, h_{i,L-1}]^T$ comprising of S_i resolvable propagation paths in the ith TDS-OFDM symbol can be modeled as [24]

$$h_{i,n} = \sum_{l=0}^{S_i-1} \alpha_{i,l}\delta[n-\tau_{i,l}], 0 \le n \le L-1, \quad (2)$$

where $\alpha_{i,l}$ is the gain of the lth path, $\tau_{i,l}$ is the delay of the lth path normalized to the sampling period at the receiver, and $h_{i,n}$ is the nth entry of the CIR vector

$$h_{i,n} = \begin{cases} \alpha_{i,l}, & n = \tau_{i,l}, \\ 0, & \text{otherwise.} \end{cases} \quad (3)$$

The path delay set D_i is defined as

$$D_i = \{\tau_{i,0}, \tau_{i,1}, \cdots, \tau_{i,S_i-1}\}, \quad (4)$$

where $0 \le \tau_{i,0} < \tau_{i,1} < \cdots < \tau_{i,S_i-1} \le L-1$ can be assumed without loss of generality, and $L \le M$ is assumed to avoid IBI between two adjacent data blocks [8]. Numerous theoretical analyses and experimental results have confirmed that the wireless channels are sparse in nature, i.e., the CIR dimension L can be large, but the number of active paths with significant power is usually small (i.e., $S_i \ll L$), especially in broadband wireless communications [20], [25], [26].

On the other hand, practical wireless channels display temporal correlations even when they are varying fast. It has been observed that the path delays vary much slower than the path gains [27], [28], i.e., even if the path gains are varying significantly from one symbol to the next symbol, the path delays during several successive symbols typically remain unchanged. This is caused by the fact that the coherence time of fast time-varying path gains is inversely proportional to the system's carrier frequency, while the duration for path delay variation is inversely proportional to the signal bandwidth [27]. For example, for a wireless broadcasting system DTMB working at 770 MHz with a signal bandwidth of 7.56 MHz [7], the path delays vary at a rate that is about 100 times slower than that of the path gains. Fig. 2 depicts snapshots of the CIRs for adjacent TDS-OFDM symbols in the Rayleigh fading Vehicular B channel [29] with a velocity of 120 km/h, whereby the channel taps are calculated based on paths delays of the Vehicular B channel model and the system bandwidth 7.56 MHz. It is clear that the locations of the nonzero taps for several consecutive CIRs remain unchanged although significant variation of path gains can be observed. This channel property is referred as "*inter-channel correlation*" in the sequel. More specifically, the CIRs for R consecutive TDS-OFDM symbols can be assumed to share the same sparsity pattern [30], i.e.,

$$\begin{cases} S_i = S_{i+1} = \cdots = S_{i+R-1} = S, \\ D_i = D_{i+1} = \cdots = D_{i+R-1} = D, \\ \tau_{i,l} = \tau_{i+1,l} = \cdots = \tau_{i+R-1,l} = \tau_l, \end{cases} \quad (5)$$

where $0 \le l \le S-1$. We define

$$\mathbf{H} = [\mathbf{h}_i, \mathbf{h}_{i+1}, \cdots, \mathbf{h}_{i+R-1}], \quad (6)$$

which is said to be jointly S-sparse, i.e., $\mathbf{H}$ has S nonzero rows with indices D in (5) due to the inter-channel correlation property of wireless time-varying channels.

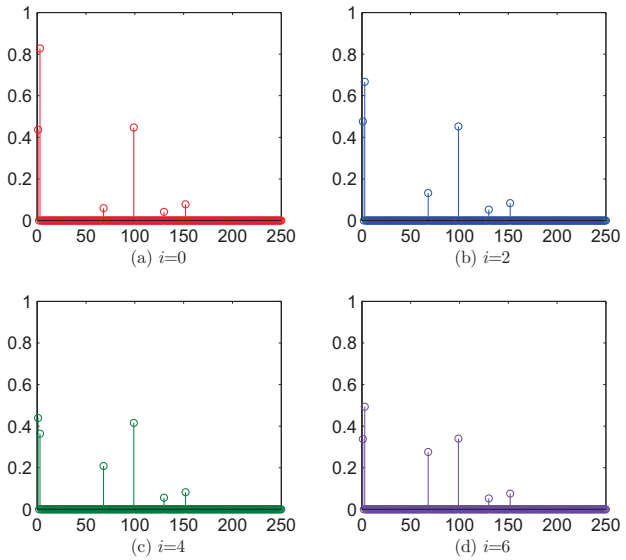

Fig. 2. Snapshot of the CIR for ith TDS-OFDM symbol in the Vehicular B channel with a velocity of 120 km/h: (a) $i = 0$; (b) $i = 2$; (c) $i = 4$; (d) $i = 6$.

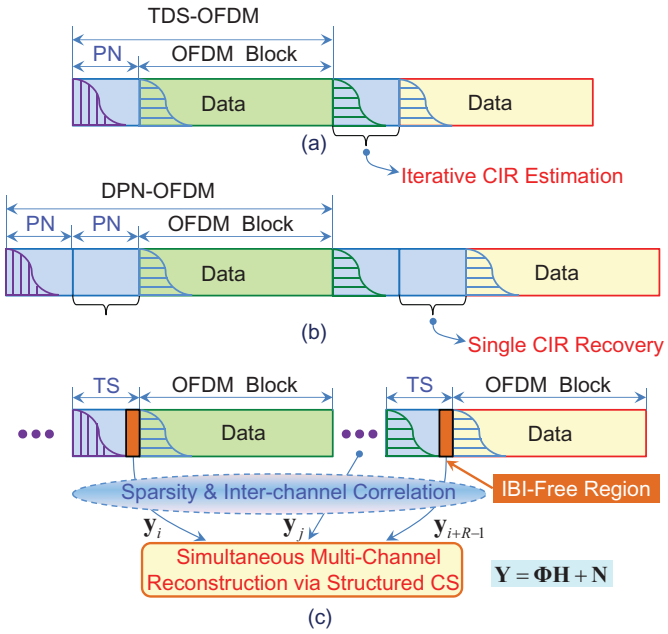

Fig. 3. The proposed SCS-aided TDS-OFDM scheme based on simultaneous multi-channel reconstruction, compared with traditional schemes: (a) The conventional TDS-OFDM scheme; (b) The dual PN padding OFDM (DPN-OFDM) scheme; (c) The proposed SCS-aided TDS-OFDM scheme.

The channel properties, in particular, the sparsity and the inter-channel correlation, which are usually not considered in conventional OFDM systems, will be fully exploited to solve the main problems of TDS-OFDM.

C. Signal Model of TDS-OFDM Based on Simultaneous Multi-Channel Reconstruction

In contrast to CP-OFDM where channel estimation is mainly based on frequency-domain pilots, TDS-OFDM performs channel estimation based on the time-domain received PN sequence $\mathbf{d}_i = [d_{i,0}, d_{i,1}, \cdots, d_{i,M-1}]^T$ denoted by

$$\mathbf{d}_i = \mathbf{\Psi}_i \mathbf{h}_i + \mathbf{v}_i, \tag{7}$$

where $\mathbf{v}_i$ is the noise term, and

$$\mathbf{\Psi}_i = \begin{bmatrix} c_{i,0} & x_{i-1,N-1} & x_{i-1,N-2} & \cdots & x_{i-1,N-L+1} \\ c_{i,1} & c_{i,0} & x_{i-1,N-1} & \cdots & x_{i-1,N-L+2} \\ c_{i,2} & c_{i,1} & c_{i,0} & \cdots & x_{i-1,N-L+3} \\ \vdots & \vdots & \vdots & \ddots & \vdots \\ c_{i,L-1} & c_{i,L-2} & c_{i,L-3} & \cdots & c_{i,0} \\ c_{i,L} & c_{i,L-1} & c_{i,L-2} & \cdots & c_{i,1} \\ \vdots & \vdots & \vdots & \ddots & \vdots \\ c_{i,M-1} & c_{i,M-2} & c_{i,M-3} & \cdots & c_{i,M-L} \end{bmatrix}.$$

As illustrated in Fig. 3 (a), in multipath channels, the received PN sequence $\mathbf{d}_i$ is contaminated by the portion $[x_{i-1,N-L+1}, x_{i-1,N-L+2}, \cdots, x_{i-1,N-1}]^T$ of the previous OFDM data block $\mathbf{x}_{i-1}$. Thus, an iterative channel estimation has to be used based on the contaminated PN sequence, whereby a reliable result is difficult to achieve in static channels with large delay spread and fast fading channels.

To solve this problem, the DPN-OFDM scheme has been proposed with two repeated PN sequences as shown in Fig. 3 (b), whereby the second PN sequence is not affected by the IBI from the previous OFDM data block and hence can be used to realize accurate channel estimation. Due to its simplicity and good performance, DPN-OFDM is currently under extensive investigation and hardware implementation for the evolution standard of DTMB [8]. However, the doubled length of the guard interval in DPN-OFDM obviously compromises the spectrum efficiency of TDS-OFDM, especially in typical application scenarios of single frequency network (SFN) for wireless broadcasting systems, whereby the original PN sequence length should be large. For example, the spectrum efficiency of 90% for TDS-OFDM is reduced to 82% for DPN-OFDM when the original length of the PN sequence is 1/9 of the OFDM data block length, which is the main working mode of the TDS-OFDM based DTMB standard [7].

In contrast to the conventional TDS-OFDM and DPN-OFDM scheme, we propose a SCS-aided TDS-OFDM scheme based on simultaneous multi-channel reconstruction as shown in Fig. 3 (c). This scheme exploits the IBI-free region $\mathbf{y}_i = [d_{i,L-1}, d_{i,L}, \cdots, d_{i,M-1}]^T$ in the last portion of the received TS for channel estimation. Such IBI-free region exists in practical systems due to the following three reasons:

1) A common rule of thumb for practical OFDM system design is to select the guard interval length M to be slightly longer than the largest expected channel delay spread M, i.e., $M > L$, so that the system performance can be still guaranteed in the worse case. For example, both the DVB-T2 standard [9] based on CP-OFDM and the DTMB standard [7] based on TDS-OFDM follow this design rule. That is to say, the IBI-free region usually exists in the received TS for practical TDS-OFDM systems due to the system design margin;

2) Depending on the terrain, distance, antenna direction and some other factors, the actual maximum channel delay spread in practical wireless systems can span from very small values to large values. For example, the guard interval length M is configured sufficiently large so that the receiver can work well even there is a long-delay path reflected from a faraway mountain, but receivers may usually work in urban areas where the maximum channel length is much smaller than M. That is to say, the actual CIR length L is usually smaller or even much smaller than the guard interval length M in practical scenarios [20];
3) Even in the extreme case that the actual CIR length L equals the guard interval length M, i.e., $L = M$, we can extend the length of the TS in the proposed TDS-OFDM scheme so that an IBI-free region can be still provided. As will be addressed later in Section IV-B, since the required size the IBI-free region is small, TS extension will only introduce negligible penalty of the spectrum efficiency (as low as 0.54% in typical applications);

Therefore, within the received TS for every TDS-OFDM symbol, we can guarantee that there is an IBI-free region of size G:

$$G = M - L + 1. \tag{8}$$

Considering the received PN sequence in (7), the IBI-free region $\mathbf{y}_i$ can be denoted as

$$\mathbf{y}_i = \mathbf{\Phi}_i \mathbf{h}_i + \mathbf{n}_i, \tag{9}$$

where $\mathbf{n}_i$ is the additive white Gaussian noise (AWGN) subject to the distribution $\mathcal{CN}(\mathbf{0}, \sigma^2 \mathbf{I}_G)$, and

$$\mathbf{\Phi}_i = \begin{bmatrix} c_{i,L-1} & c_{i,L-2} & c_{i,L-3} & \cdots & c_{i,0} \\ c_{i,L} & c_{i,L-1} & c_{i,L-2} & \cdots & c_{i,1} \\ \vdots & \vdots & \vdots & \vdots & \vdots \\ c_{i,M-1} & c_{i,M-2} & c_{i,M-3} & \cdots & c_{i,M-L} \end{bmatrix}_{G \times L} \tag{10}$$

denotes the Toeplitz matrix of size $G \times L$ determined by the time-domain TS $\mathbf{c}_i$. Note that $\mathbf{\Phi}_i$ corresponds to the last G rows of the matrix $\mathbf{\Psi}_i$ in (7).

The actual CIR length and the system design margin motivate us to use the low-dimensional IBI-free region to recover the high-dimensional CIR without iterative interference cancellation. However, since the size of the IBI-free region G is usually small, it will be impossible in the linear theory to estimate the CIR from the under-determined (and perhaps severely ill-conditioned) mathematical problem (9) if the number of observations G is smaller than the dimension of the unknown CIR $\mathbf{h}_i$, i.e., $G < L$ (or $M < 2L+1$). That is the mathematical reason why an extra PN sequence is inserted in DPN-OFDM to generate the second "pure" PN sequence of length M ($M \geq L$) to estimate the L-dimensional CIR. Fortunately, the ground-breaking CS theory [21] has proved that the high-dimensional original signal can be reconstructed from the low-dimensional observations if the signal is (approximately) sparse, i.e., the number of nonzero entries of the signal is much smaller than its dimension. Thus, the ideal of exploiting the IBI-free region of small size to accurately recover the sparse CIR of large length without iterative interference cancellation becomes feasible under the framework of the CS theory. Consequently, the mutually conditional time-domain channel estimation and frequency-domain data demodulation in conventional TDS-OFDM can be decoupled without changing the TDS-OFDM signal structure or consequently compromising the spectrum efficiency.

Furthermore, the inter-channel correlation property of wireless channels can also be exploited to improve the performance of the proposed scheme. When the same PN sequence is used by different TDS-OFDM symbols (which is usually the case in most applications adopting TS as the guard interval, including the multi-carrier TDS-OFDM scheme and the unique word single carrier (UW-SC) scheme), we have $\mathbf{c}_i = \mathbf{c}_{i+1} = \cdots = \mathbf{c}$, and hence $\mathbf{\Phi}_i = \mathbf{\Phi}_{i+1} = \cdots = \mathbf{\Phi}$. Then, considering the IBI-free regions of R consecutive TDS-OFDM symbols as well as the signal model (9), we have

$$\mathbf{Y} = [\mathbf{y}_i, \mathbf{y}_{i+1}, \cdots, \mathbf{y}_{i+R-1}]_{G \times R} = \mathbf{\Phi}\mathbf{H} + \mathbf{N}, \tag{11}$$

where $\mathbf{N} = [\mathbf{n}_i, \mathbf{n}_{i+1}, \cdots, \mathbf{n}_{i+R-1}]_{G \times R}$ denotes the AWGN matrix, and the columns of $\mathbf{H}$ share the same locations of nonzero elements, so the support (indices of nonzero rows) of the matrix $\mathbf{H}$ is just D in (5). The formulated mathematical model (11) precisely complies with the newly developed theory of SCS [31], which is an extension of the standard CS theory [21].

Under the framework of SCS theory, the jointly sparse multiple CIRs within $\mathbf{H}$ can be simultaneously reconstructed by solving the following nonlinear optimization problem [31]:

$$\widehat{\mathbf{H}} = \arg \min_{\mathbf{H} \in \mathbf{C}^{L \times R}} \|\mathbf{H}\|_{p,q}, \quad \text{subject to } \|\mathbf{Y} - \mathbf{\Phi}\mathbf{H}\|_{p,q} \leq \xi^2, \tag{12}$$

where ξ^2 denotes the impact of the unknown noise $\mathbf{N}$ on the signal recovery accuracy, $l_{p,q}$ norm of the matrix $\mathbf{H}$ is defined as

$$\|\mathbf{H}\|_{p,q} = \left(\sum_i \|\mathbf{H}_i\|_p^q \right)^{\frac{1}{q}}, \tag{13}$$

with $\mathbf{H}_i$ being the ith row of $\mathbf{H}$. Typically an $l_{2,0}$ norm is used in the CS literature [31], and in this case $\xi^2 = R\sigma^2$. Note that standard CS without exploiting the inter-channel correlation can be regarded as a special case of SCS with $R = 1$ in (11) and (12). The required number of observations for reliable signal reconstruction will be reduced from $\mathcal{O}(S\log_2(L/S))$ for standard CS to $\mathcal{O}(S)$ for SCS [30], which indicates that a smaller IBI-free region will be required by the proposed SCS-aided TDS-OFDM based on multi-channel reconstruction.

A reliable yet low-complexity solution to (12) is essential to realize the proposed SCS-aided TDS-OFDM scheme, which is the topic of the following section.

III. Simultaneous Multi-Channel Reconstruction Based on A-SOMP

Several signal reconstruction algorithms in standard CS theory have been extended to the SCS framework to achieve jointly sparse signals reconstruction [30], [31]. Among them, SOMP derived from the well-known OMP algorithm has drawn extensive attention due to its satisfying reconstruction

quality [22]. The key idea of SOMP is to find the solution to (12) by sequentially selecting a small subset of column vectors of $\mathbf{\Phi}$ to approximate the observation matrix $\mathbf{Y}$ in an iterative manner. However, SOMP requires in advance the known sparsity level S and the number of observations, both of which will be variable and unavailable in practical applications. Moreover, since matrix inversion is required in each iteration step, SOMP has a high computational complexity for hardware implementation.

To alleviate these problems of SOMP, we propose an adaptive SOMP (A-SOMP) algorithm based on the basic principle of SOMP, whereby the specific features of TDS-OFDM are also exploited to obtain a partial priori information of the channel, which includes the estimated sparsity level, CIR length, and partial support of the channel. These information can be used by the A-SOMP algorithm to reduce the computational complexity as well as to make it adaptive to the channel variation. We then propose an A-SOMP based simultaneous multi-channel reconstruction scheme comprising the following three steps: 1) Correlation based partial CIR priori acquisition; 2) A-SOMP based joint sparsity pattern recovery; 3) Least square (LS) based path gain estimation.

A. Correlation Based Partial CIR Priori Acquisition

Although the proposed SCS-aided TDS-OFDM scheme mainly relies on multiple IBI-free regions within the received TSs for simultaneous multi-channel reconstruction, the complete received TSs (including the parts contaminated by the OFDM data blocks) can still be utilized to acquire a part of the CIR priori information.

Relying on the good auto-correlation properties of the TS[3], without IBI removal, the contaminated TS at the receiver can be directly correlated with the locally known TS to generate a first CIR estimate $\overline{\mathbf{h}}_i$:

$$\overline{\mathbf{h}}_i = \frac{1}{M}\mathbf{c}_i \otimes \mathbf{d}_i = \mathbf{h}_i + \mathbf{u}_i, \tag{14}$$

where $\mathbf{u}_i$ corresponds to the AWGN as well as the IBI effect caused by the previous OFDM data block.

Although we are not expecting a reliable CIR estimate due to the absence of IBI removal, as illustrated in Fig. 4 where the Vehicular B channel [29] with a low signal-to-noise ratio (SNR) of 5 dB is considered, the good auto-correlation properties of the TS ensure that the main characteristics of the CIR, particularly the path delay information, can be preserved by the correlation-based first CIR estimate (14).

Based on the first CIR estimates $\overline{\mathbf{h}}_i$ during several consecutive TDS-OFDM symbols, the number of observation vectors R needed to generate the observation matrix $\mathbf{Y}$ in (11) can be determined by checking the locations of the most significant taps within these CIR estimates. Then, the path gains in $\overline{\mathbf{h}}_i$ are discarded, and the initial partial support of the jointly sparse CIRs can be approximated by

$$D_0 = \{l : \sum_{j=i}^{i+R-1} \left|\overline{h}_{j,l}\right|^2 > p_{th}\}_{l=0}^{L-1}, \tag{15}$$

[3]Note that synchronization in TDS-OFDM also relies on the good auto-correlation properties of the TS [8].

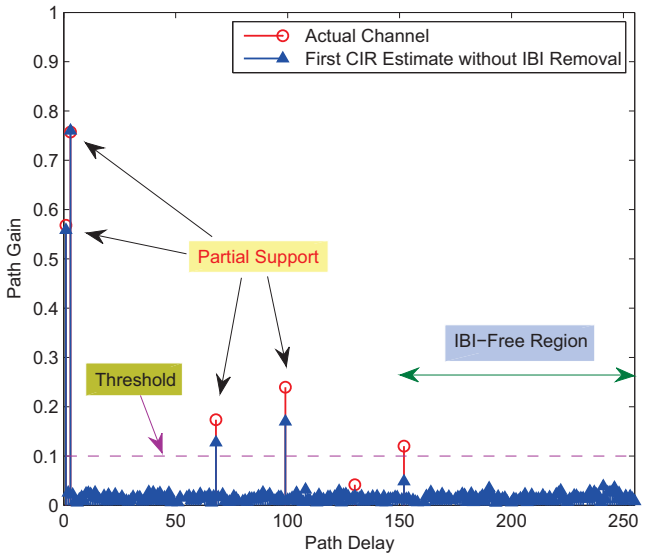

Fig. 4. CIR priori acquisition by directly using the contaminated TS without IBI removal in the Vehicular B channel with a low SNR of 5 dB.

where p_{th} is a power threshold used to determine the active paths, which can be configured conservatively larger than that in [32] to ensure the correct information of the obtained partial support, e.g, $p_{th} = 0.1$ is used in Fig. 4.

The channel sparsity level S is then estimated by

$$S = S_0 + a = \|D_0\|_0 + a, \tag{16}$$

where $S_0 = \|D_0\|_0$ denotes the number of nonzero elements in D_0, which corresponds to the initial channel sparsity level according to the first CIR estimates, and a is a positive number used to combat the interference effect, since some low-gain active paths maybe treated as noise in (15).

Finally, the CIR length L can be estimated by

$$\widehat{L} = \max\{D_0\} + b, \tag{17}$$

where b is a variable parameter used to define the IBI-free region comprising the last G samples of the received TS. It is worth noting that the CS theory can also be utilized to reduce the pilot overhead in CP-OFDM systems [25], [26], but the partial CIR priori can be obtained in TDS-OFDM is usually unavailable in CP-OFDM. The partial CIR priori is essential for the reduced computational complexity of the proposed A-SOMP algorithm in the next subsection.

B. A-SOMP Based Joint Sparsity Pattern Recovery

Based on the basic principle of SOMP, we propose the A-SOMP algorithm adaptive to the channel variation, and the partial CIR priori obtained in TDS-OFDM can be exploited to reduce the computational complexity of the original SOMP algorithm. The pseudocode of the proposed A-SOMP algorithm is provided in Algorithm 1, which differs from SOMP [22] in the following three aspects:

1) **Number of iterations**. Since the partial support is already known, A-SOMP executes $S - S_0$ iterations

Input: 1) Initial support D_0, initial channel sparsity level S_0, estimated channel sparsity level S;
2) Noisy measurements $\mathbf{Y}$, observation matrix $\mathbf{\Phi}$.
Output: S-sparse estimate $\widehat{\mathbf{H}}$ containing multiple CIRs.
$\Omega \leftarrow D_0$;
$k \leftarrow S_0$;
$\widehat{\mathbf{H}}_k\Big|_{\Omega} \leftarrow \mathbf{\Phi}_{\Omega}^{\dagger}\mathbf{Y}$;
$\mathbf{R} \leftarrow \mathbf{Y} - \mathbf{\Phi}\widehat{\mathbf{H}}_k\Big|_{\Omega}$;
while $k \leq S$ **do**
  $k \leftarrow k+1$;
  $\mathbf{E} \leftarrow \mathbf{\Phi}^H\mathbf{R}$;
  $\Gamma \leftarrow \arg\max_k \sum_j |e_{k,j}|$;
  $\Omega \leftarrow \Omega \cup \Gamma$;
  $\widehat{\mathbf{H}}_k\Big|_{\Omega} \leftarrow \mathbf{\Phi}_{\Omega}^{\dagger}\mathbf{Y}$, $\widehat{\mathbf{H}}_k\Big|_{\Omega^c} \leftarrow \mathbf{0}$;
  $\mathbf{R} \leftarrow \mathbf{Y} - \mathbf{\Phi}\widehat{\mathbf{H}}_k$;
end
$\widehat{\mathbf{H}} \leftarrow \widehat{\mathbf{H}}_k$;

Algorithm 1: Adaptive SOMP (A-SOMP)

instead of S iterations in SOMP. This leads to a reduced computational complexity if most of the CIR support has been obtained from the correlation based first CIR estimation.

2) **Initialization**. The initial support is set to $\Omega \leftarrow D_0$ in A-SOMP instead of $\Omega \leftarrow \mathbf{0}$ in SOMP, the initial residual signal $\mathbf{R} \leftarrow \mathbf{Y} - \mathbf{\Phi}$ is used to replace its counterpart $\mathbf{R} \leftarrow \mathbf{0}$ in SOMP, whereby $\mathbf{\Phi}_{\Omega}^{\dagger}\mathbf{Y}$ is the initial estimate of the channel.
3) **Adaptivity**: Since the inputs of A-SOMP can vary in different channel conditions, the proposed A-SOMP algorithm is adaptive to the channel sparsity level S, the number of observation vectors R, as well as the size of the IBI-free region G, etc. Such adaptivity is preferred for practical systems where better performance is expected when the channel condition becomes good.

After $\widehat{\mathbf{H}}$ has been obtained by the proposed A-SOMP algorithm, again the path gains within $\widehat{\mathbf{H}}$ are discarded, and the path delays of the nonzero taps can be obtained by the support of $\widehat{\mathbf{H}}$ as follows

$$D = \text{supp}\{\widehat{\mathbf{H}}\}. \tag{18}$$

Unlike conventional SCS algorithms where both the locations of nonzero taps and the corresponding gains are considered, we only utilize the A-SOMP algorithm to acquire the joint path delays of the multiple channels, while the path gains are estimated in the third step as explained in the next subsection.

C. LS Based Path Gain Estimation

After the path delays have been obtained, the signal model (9) is simplified to

$$\mathbf{y}_i = \mathbf{\Phi}_D\mathbf{h}_{iS} + \mathbf{n}_i, \tag{19}$$

where $\mathbf{h}_{iS}$ is generated by restricting the vector $\mathbf{h}_i$ to its S largest components. It is clear from (19) that there remain only S instead of L ($S < G \ll L$) unknown nonzero path gains in the CIR vector $\mathbf{h}_i$, which can be estimated by solving an over-determined set of equations under the LS criterion:

$$\widehat{\mathbf{h}}_{iS} = \mathbf{\Phi}_D^{\dagger}\mathbf{y}_i = \left(\mathbf{\Phi}_D{}^H\mathbf{\Phi}_D\right)^{-1}\mathbf{\Phi}_D{}^H\mathbf{y}_i. \tag{20}$$

Finally, the path delay and path gain estimates form the complete CIR estimate as $\widehat{\mathbf{h}}_i\Big|_D = \widehat{\mathbf{h}}_{iS}$.

Similar operation (20) can be carried out to obtain the estimates of the remaining $R-1$ CIR vectors to finally accomplish the simultaneous multi-channel reconstruction.

IV. Performance Analysis

This section presents the performance analysis of the proposed scheme including the derivation of the Cramér-Rao lower bound (CRLB) of the simultaneous multi-channel reconstruction method based on A-SOMP, as well as the spectrum efficiency, the energy efficiency, and the computational complexity.

A. CRLB of Simultaneous Multi-Channel Reconstruction

According to the signal model (19) where the AWGN vector $\mathbf{n}$ (the subscript i of $\mathbf{n}_i$, $\mathbf{h}_i$, and $\mathbf{y}_i$ is omitted in this subsection for sake of conciseness) follows a complex normal distribution $\mathcal{CN}(\mathbf{0}, \sigma^2\mathbf{I}_G)$, the conditional probability density function (PDF) of $\mathbf{y}$ with the given $\mathbf{h}_S$ is

$$p_{\mathbf{y}|\mathbf{h}_S}(\mathbf{y};\mathbf{h}_S) = \frac{1}{(2\pi\sigma^2)^{G/2}}\exp\left\{-\frac{1}{2\sigma^2}\|\mathbf{y}-\mathbf{\Phi}_D\mathbf{h}_S\|_2\right\}. \tag{21}$$

The Fisher information matrix [33] of (21) can be then derived as

$$[\mathbf{J}]_{i,j} \triangleq -\text{E}\left\{\frac{\partial^2 \ln p_{\mathbf{y}|\mathbf{h}_S}(\mathbf{y};\mathbf{h}_S)}{\partial h_{S,i}\partial h_{S,j}}\right\} = \frac{1}{\sigma^2}\left[(\mathbf{\Phi}_D)^H\mathbf{\Phi}_D\right]_{i,j}, \tag{22}$$

where $h_{S,i}$ and $h_{S,j}$ present the ith and jth elements of $\mathbf{h}_S$, respectively. Thus, according to the vector estimation theory [33], we have

$$\begin{aligned}\text{CRLB} &= \text{E}\left\{\left\|\widehat{\mathbf{h}}_S - \mathbf{h}_S\right\|_2\right\} \geq \text{Tr}\left\{\mathbf{J}^{-1}\right\} \\ &= \sigma^2\text{Tr}\left\{\left(\mathbf{\Phi}_D^H\mathbf{\Phi}_D\right)^{-1}\right\}.\end{aligned} \tag{23}$$

Let $\{\lambda_i\}_{i=1}^S$ be the S eigenvalues of the matrix $\mathbf{\Phi}_D^H\mathbf{\Phi}_D$, then, we have the following result according to the elementary linear algebra

$$\begin{aligned}\text{Tr}\left\{\left(\mathbf{\Phi}_D^H\mathbf{\Phi}_D\right)^{-1}\right\} &= \sum_{i=1}^{S}\lambda_i^{-1} = S\left(\sum_{i=1}^{S}\lambda_i^{-1}/S\right) \\ &\overset{(z)}{\geq} S\left(S/\sum_{i=1}^{S}\lambda_i\right) = \frac{S^2}{\text{Tr}\left\{\mathbf{\Phi}_D^H\mathbf{\Phi}_D\right\}},\end{aligned} \tag{24}$$

where the arithmetic-harmonic means inequality [34] denoted by (z) has been utilized. The equality holds if and only if $\lambda_1 = \lambda_2 = \cdots = \lambda_S$, which means that the matrix $\mathbf{\Phi}_D$ extracted from the observation matrix $\mathbf{\Phi}$ should have orthogonal columns. In this case, the $S \times S$ matrix $\mathbf{\Phi}_D^H\mathbf{\Phi}_D$ has identical diagonals equal to G, i.e., $\text{Tr}\left\{\mathbf{\Phi}_D^H\mathbf{\Phi}_D\right\} = GS$. Finally, the

CRLB of the proposed multi-channel reconstruction method becomes

$$\mathrm{CRLB} = \frac{S\sigma^2}{G}. \tag{25}$$

Compared with conventional TDS-OFDM with PN-based iterative channel estimation, whereby the best mean square error (MSE) performance is σ^2 (the noise level) if mutual interference can be completely removed (such MSE performance can be directly achieved by DPN-OFDM because no interference is imposed on the second PN sequence), the simultaneous multi-channel reconstruction method based on A-SOMP achieves a much better MSE performance, since S is smaller or even much smaller than G, i.e., $S < G$.

Note that if the matrix $\mathbf{\Phi}_D$ does not have orthogonal columns, the CRLB (25) cannot be achieved in practice. However, due to the good auto-correlation properties of the PN sequence used in TDS-OFDM as well as the random locations of active paths of wireless channels, the matrix $\mathbf{\Phi}_D$ has imperfect but approximately orthogonal columns[4], so the CRLB can be asymptotically approached, which will be validated by the simulation results in Section V.

B. Spectrum Efficiency

The normalized spectrum efficiency γ_0 of the considered OFDM schemes compared with the ideal OFDM scheme without any overhead (i.e., no time-domain guard interval and no frequency-domain pilots) is [8]

$$\gamma_0 = \frac{N_{\mathrm{data}}}{N_{\mathrm{data}} + N_{\mathrm{pilot}}} \times \frac{N}{N+M} \times 100\%, \tag{26}$$

where N_{data} and N_{pilot} denote the number of data subcarriers and pilot subcarriers, respectively.

Table I compares the spectrum efficiency of the proposed scheme with the conventional OFDM schemes in typical wireless broadcasting applications with the 4K mode ($N = 4096$) when the same constellation is used. It is clear that the proposed scheme has the highest spectrum efficiency identical to that of the conventional TDS-OFDM scheme, and outperforms CP-OFDM by more than 10% in typical applications ($M = N/16$). In addition, as will be demonstrated later in Section V that the proposed SCS-aided TDS-OFDM scheme can support 256QAM in realistic static channels with large delay spread, while the conventional TDS-OFDM scheme can only support 64QAM in such scenarios, we can obtain a higher spectrum efficiency by about 30% than the current TDS-OFDM based DTMB standard without changing the signal structure.

As mentioned in Section II-C that in the extreme case that the actual CIR length L equals the guard interval length M, we can extend the TS in the proposed TDS-OFDM scheme so that an IBI-free region can be still provided. Note that such TS extension will reduce the spectrum efficiency. However, as has been theoretically addressed in Section II-C that only $\mathcal{O}(S)$ observations ($S \ll L$) are required to recover a length-L CIR based on the SCS theory, the loss in spectrum efficiency will be negligible. This can be further quantified later in Section V that only an IBI-free region of length 25 is sufficient to provide accurate multi-channel reconstruction when $L = M = N/16 = 256$, which means that the original length-256 TS should be extended by only 25 samples to obtain the necessary IBI-free region. The corresponding spectrum efficiency will be reduced from 94.12% to 93.58%, which corresponds to a negligible spectrum efficiency penalty as small as 0.54%.

[4]The requirement of near orthogonality is equivalent to the restricted isometry property (RIP) of the observation matrix widely studied in the CS theory, and the performance guarantee of the Toeplitz observation matrix has been theoretically proved in [35].

TABLE I
SPECTRAL EFFICIENCY COMPARISON.

	CP-OFDM[a]	TDS-OFDM	DPN-OFDM	Proposed Scheme
$M = N/4$	70.97%	80.00%	66.67%	80.00%
$M = N/8$	78.85%	88.89%	80.00%	88.89%
$M = N/16$	83.49%	94.12%	88.89%	94.12%

[a] We consider the typical example that the pilot occupation ratio in CP-OFDM is about 11.29%, which is specified by the 4K mode of the DVB-T2 standard [9].

C. Energy Efficiency

The energy efficiency η_0 of the considered OFDM schemes is

$$\eta_0 = \frac{N_{\mathrm{data}}}{N_{\mathrm{data}} + \beta^2 N_{\mathrm{pilot}}} \times \frac{N}{N+\alpha^2 M} \times 100\%, \tag{27}$$

where β and α denote the amplitude factor imposed on the frequency-domain pilots and time-domain guard interval, respectively. Pilot amplitude boosting is usually adopted by CP-OFDM to enhance the receiver performance, e.g., $\beta = 4/3$ has been specified by the DVB-T2 standard [9]. Similarly, the amplitude of the PN sequence is boosted in TDS-OFDM to ensure a reliable channel estimation, e.g., $\alpha = \sqrt{2}$ has been specified by the DTMB standard [7]. On the contrary, since it has been theoretically proved in Section IV-A that the proposed SCS-aided TDS-OFDM scheme can provide obviously improved channel estimation performance, we propose to decrease the TS amplitude to further improve the energy efficiency. Note that boosting of the guard interval amplitude is infeasible for CP-OFDM systems.

Table II summarizes the energy efficiency comparison for different OFDM schemes. It is clear that in typical applications when $M = N/16$, the conventional TDS-OFDM already has about 12% higher energy efficiency than CP-OFDM, and the proposed scheme has the highest energy efficiency, which outperforms CP-OFDM by more than 20%.

D. Computational Complexity

The computational complexity of the proposed simultaneous multi-channel reconstruction scheme in terms of the required number of complex multiplications includes the following three parts:

1) In the first step of correlation based partial CIR priori acquisition (14), the complexity $\mathcal{O}(M)$ is required for every TDS-OFDM symbol.

TABLE II
ENERGY EFFICIENCY COMPARISON.

	CP-OFDM[a]	TDS-OFDM[b]	DPN-OFDM[c]	Proposed Scheme
$M = N/4$	65.23%	66.67%	66.67%	88.89%
$M = N/8$	72.48%	80.00%	80.00%	94.12%
$M = N/16$	76.75%	88.89%	88.89%	96.97%

[a] We consider the typical example that the pilot occupation ratio in CP-OFDM is about 11.29%, which is specified by the 4K mode of the DVB-T2 standard [9].
[b] The amplitude factor is $\alpha = \sqrt{2}$ as specified by DTMB standard [7].
[c] The amplitude factor is $\alpha = 1$ according to [19].

2) In the second step of A-SOMP based joint sparsity pattern recovery (see Algorithm 1 in Section III-B), for each iteration, the inner product between the residual $\mathbf{R}$ and the observation matrix $\mathbf{\Phi}$ has the complexity $\mathcal{O}(RGL)$, and solving multiple LS problems $\widehat{\mathbf{H}}_k\big|_{\Omega} \leftarrow \mathbf{\Phi}_{\Omega}^{\dagger}\mathbf{Y}$ can be implemented with the complexity in the order of $\mathcal{O}(RGS^2)$ when using the Gram-Schmidt algorithm (note that although the size of the observation matrix $\mathbf{\Phi}$ maybe large, the linear LS problem only uses a submatrix of $\mathbf{\Phi}$ whose size is not larger than $G \times S$). Thus, the total complexity of the A-SOMP algorithm with $S-S_0$ iterations is $\mathcal{O}((S-S_0)RG(L+S^2))$. As has been addressed in Section III-B, compared to SOMP, the proposed A-SOMP algorithm reduces the computational complexity by a factor of S_0/S, which means that the computational complexity is reduced by about 66.67% if four out of six channel path delays have been obtained by the first step of partial CIR priori acquisition.
3) In the third step of LS based path gain estimation (20), the complexity is $\mathcal{O}(GS^2)$ for each TDS-OFDM symbol.

To sum up, the total complexity is $\mathcal{O}(RM + (S - S_0)RG(L + S^2) + RGS^2)$ for R consecutive TDS-OFDM symbols. As $S \ll L \leq M$, the proposed simultaneous multi-channel reconstruction scheme has the computational complexity in the order of $\mathcal{O}((S - S_0)RGL)$.

V. SIMULATION RESULTS AND DISCUSSION

Extensive simulations have been carried out to investigate and validate the performance of the proposed SCS-aided TDS-OFDM scheme based on simultaneous multi-channel reconstruction. The simulation setup is configured according to the typical wireless broadcasting systems [7]. The signal bandwidth is 7.56 MHz located at the central radio frequency of 770 MHz. A DFT size $N = 4096$ and a guard interval length $M = 256$ are adopted. The bit interleaved coding and modulation (BICM) scheme with a bit interleaver between channel coding and constellation mapping as specified in the DVB-T2 standard [9] is considered. Specifically, the powerful low-density parity-check (LDPC) code with a block length 64, 8000 bits and a code rate 0.6 and the modulation schemes 256QAM and 64QAM as specified in [9] are adopted. The six-tap Vehicular B channel model [29] with a large delay spread of 20 μs defined by 3GPP is considered[5], whereby a receiver velocity of 120 km/h is used to model the fast fading channels. $R = 10$ consecutive TDS-OFDM symbols are used for simultaneous multi-channel reconstruction.

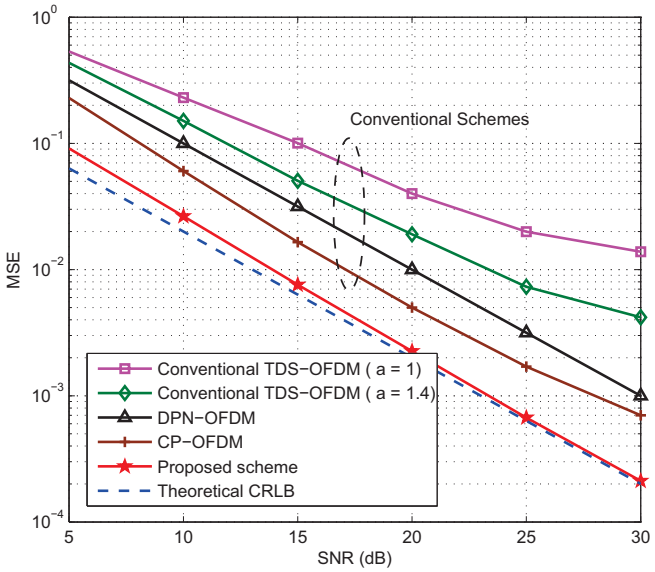

Fig. 5. Channel estimation performance comparison in a static Vehicular B channel with large delay spread.

Fig. 5 shows the channel estimation performance comparison between the proposed scheme and the conventional TDS-OFDM, DPN-OFDM, and CP-OFDM schemes in a static Vehicular B channel. To ensure the channel estimation performance when the SNR is low[6], the size of the IBI-free region is selected as $G = 30$ for the simultaneous multi-channel reconstruction. For the conventional TDS-OFDM scheme, the iterative interference cancellation with the number of iterations equal to three is carried out to achieve time-domain channel estimation [11], while the second received PN sequence is directly used for channel estimation in the DPN-OFDM scheme [19]. For the CP-OFDM scheme as specified by DVB-T2 [9], the pilots are used to acquire the CFR at the corresponding frequency-domain subcarriers, and then the robust Wiener filtering scheme [15] with low-complexity but satisfying performance is used to obtain the CFR over the entire signal bandwidth. It is clear from Fig. 5 that the proposed scheme outperforms the conventional TDS-OFDM and DPN-OFDM schemes by more than 5 dB when a target MSE of 10^{-2} is considered. Moreover, the actual MSE performance approaches the theoretical CRLB (25) when the SNR becomes high. The accurate channel estimation is mainly contributed by the fact that the sparsity as well as the inter-

[5]Note that other channel models defined by 3GPP and the channel models defined for terrestrial digital television system evaluation [8] have a samll number of active paths.

[6]Since the previous literature [12]–[17], [19], [20], [36] adopt SNR as the metric, in this section we also use SNR instead of E_b/N_0 for direct comparison between our proposal and the conventional schemes. Note that SNR relates to E_b/N_0 via SNR $= E_bR_b/N_0B$, where R_b/B is the system spectrum efficiency (refer to page 57 of [37].

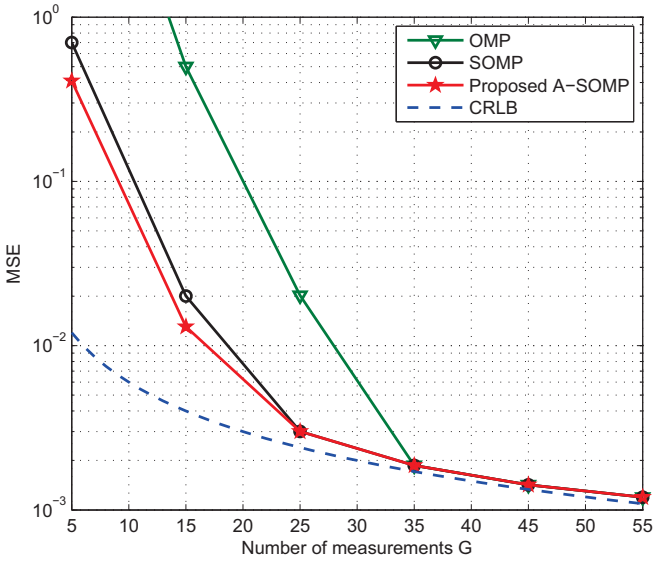

Fig. 6. Reconstruction performance comparison between the proposed A-SOMP algorithm and the conventional OMP and SOMP algorithms when a varying number of measurements G is used in the static Vehicular B channel.

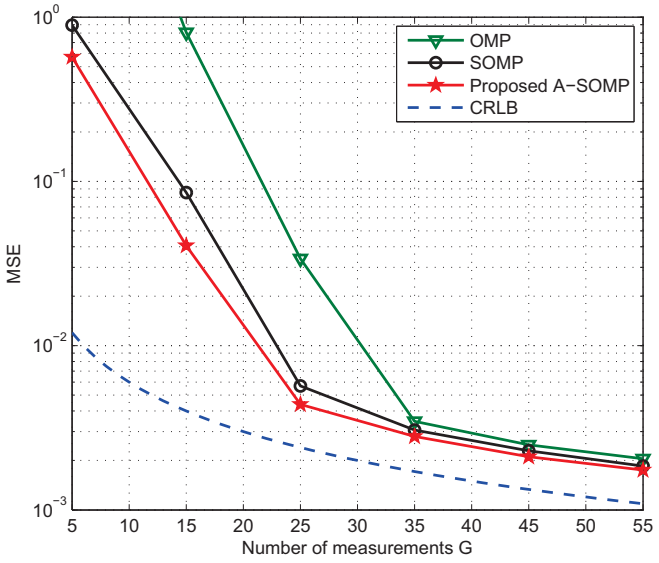

Fig. 8. Reconstruction performance comparison between the proposed A-SOMP algorithm and the conventional OMP and SOMP algorithms in a Vehicular B channel with a velocity of 120 km/h.

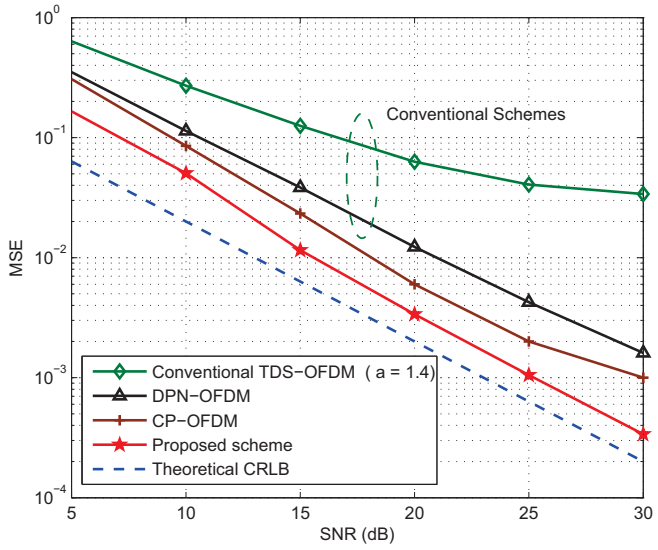

Fig. 7. Channel estimation performance comparison in a Vehicular B channel with a velocity of 120 km/h.

channel correlation of the channels are fully exploited.

Fig. 6 presents the reconstruction performance comparison between the proposed A-SOMP algorithm and the traditional SOMP algorithm when a varying number of measurements G as indicated by (8) is used in the static Vehicular B channel. The widely investigated OMP algorithm from the standard CS literature is also considered for comparison. Compared to OMP, both SOMP and A-SOMP require fewer observations to achieve the same reconstruction quality when the observation number is small, e.g., $G < 35$, since several observation vectors are utilized by SOMP and A-SOMP while only one vector is used by OMP. The direct favorable impact of the reduced number of required observations is that, the size of the IBI-free region could be smaller, and hence a longer maximum CIR length can be combatted by the proposed SCS-aided TDS-OFDM scheme. When the number of observations is large (e.g., $G \geq 35$), OMP already provides reliable performance and no gain can be achieved by SOMP and A-SOMP. The simulation results coincide with the theoretical results in [31], since all the CIR vectors in $\mathbf{H}$ are identical in static channels, and the rank of $\mathbf{H}$ is 1, so there exists no advantage for joint processing. Meanwhile, A-SOMP performs slightly better than SOMP because the partial CIR priori has been used. Note that the partial CIR priori is mainly used to reduce the computational complexity of SOMP as discussed in Section III-B. Moreover, it is clear that the reconstruction quality approaches the theoretical CRLB when the number of observations becomes large.

As the counterparts of Figs. 5 and 6 where a realistic static channel is considered, Figs. 7 and 8 present the MSE performance comparison in a fast block fading Vehicular B channel with a velocity of 120 km/h. We can observe that the MSE performance is degraded for all considered schemes, especially for conventional TDS-OFDM scheme where the mutual interference severely deteriorates the system performance in fast time-varying channels. However, compared with conventional TDS-OFDM and DPN-OFDM schemes, the proposed solution still has a SNR gain of more than 5 dB in this case, and the MSE is as small as 3.4×10^{-3} when the receiver SNR is 20 dB. We also find that the proposed A-SOMP algorithm performs slightly better than SOMP in fast fading channels, and they both have a better MSE performance than OMP.

Fig. 9 compares the coded BER performance when

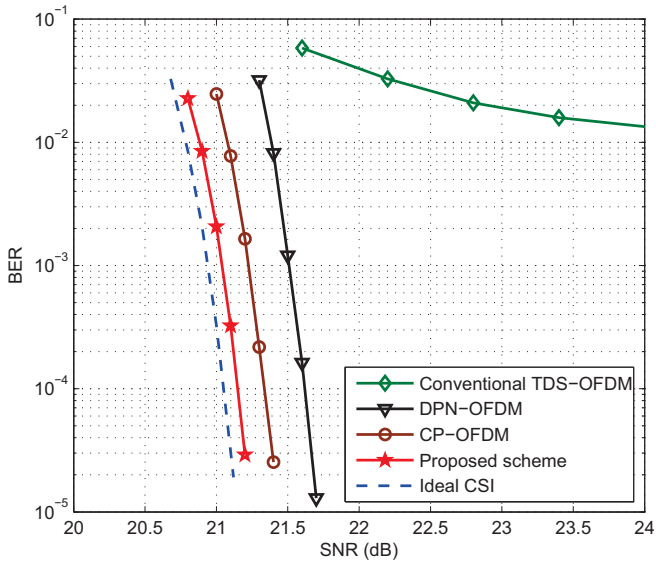

Fig. 9. BER performance comparison when 256QAM is adopted in a static Vehicular B channel.

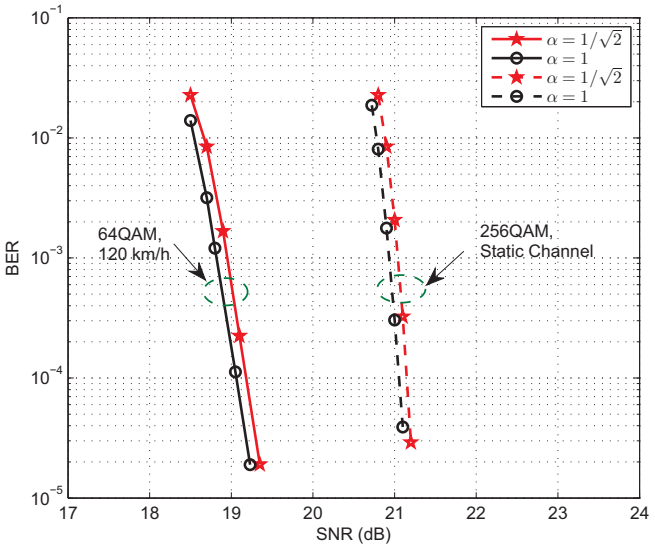

Fig. 11. The impact of decreased amplitude of the guard interval on the system BER performance.

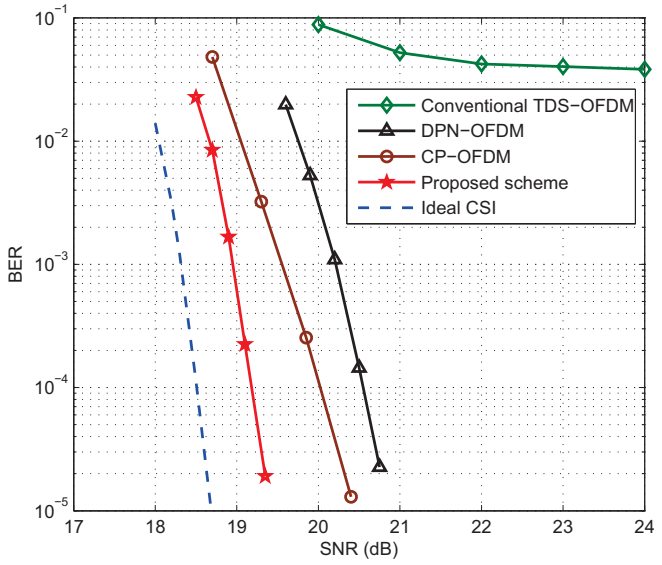

Fig. 10. BER performance comparison when HDTV is delivered (64QAM together with the LDPC code rate of 0.6) in a fast fading Vehicular B channel with a velocity of 120 km/h.

256QAM is adopted in a static Vehicular B channel. The BER performance with the ideal channel state information (CSI) is also included as the benchmark for comparison. We observe that the conventional TDS-OFDM scheme cannot support 256QAM because the mutual interference between the TS and OFDM data block cannot be removed well. However, the proposed SCS-aided TDS-OFDM scheme can support 256QAM reliably, since very accurate channel estimation as demonstrated by Fig. 5 can be used to efficiently remove the mutual interference. Moreover, owing to the decoupling of the time-domain channel estimation and frequency-domain data detection, as well as the high channel estimation accuracy, the proposed scheme also has a better BER performance than DPN-OFDM and CP-OFDM with an SNR gain of about 0.5 dB and 0.2 dB at a BER of 1×10^{-4}, respectively. In addition, the actual BER curve is only about 0.1 dB away from the ideal CSI case, which indicates the excellent channel estimation performance of the proposed scheme. It should be pointed out that although both DPN-OFDM and CP-OFDM can also support 256QAM, their spectrum and energy efficiency are lower than those of the proposed scheme.

Fig. 10 shows the BER performance comparison when 64QAM modulation and the LDPC code rate of 0.6 are configured, which is the primary working mode of DTMB to provide HDTV services with a data rate of 24.4 Mbps [7]. It is known that reliable HDTV delivery can be achieved over static or low-speed channels, but it is highly expected that HDTV can also be delivered in high-speed vehicles. From Fig. 10, we can observe that the conventional TDS-OFDM scheme cannot support HDTV delivery in fast fading channels, whereby the inaccurate channel estimation as shown in Fig. 7 cannot be used for reliable mutual interference cancellation and data demodulation. However, the proposed scheme can achieve reliable HDTV delivery with a BER performance only 0.5 dB away from the ideal CSI case. We can also find that the proposed scheme outperforms DPN-OFDM and CP-OFDM by a SNR gain of 1.4 dB and 0.8 dB at a BER of 1×10^{-4}, respectively. Again, it is worthwhile to note that the spectrum and energy efficiency of the proposed scheme are higher than those of DPN-OFDM and CP-OFDM, although the latter two schemes can also support HDTV delivery in fast fading channels.

Finally, the impact of different TS amplitudes on the system BER performance is evaluated in Fig. 11. As has been

discussed in Section IV-C, in contrast to the conventional TDS-OFDM scheme which boosts the TS amplitude to guarantee the receiver performance, the TS amplitude can be decreased in the proposed scheme to further improve the energy efficiency. Compared to the case when $\alpha = 1$, we can observe that a negligible SNR loss will be introduced when $\alpha = 1/\sqrt{2}$, e.g., the SNR loss is less than 0.1 dB both in a static and a fast fading channel. Although decreasing the TS amplitude results in a reduced MSE performance of the simultaneous multi-channel reconstruction, the channel estimate is still accurate enough for reliable cancellation of the mutual interference and data demodulation.

VI. Conclusions

In this paper, we have developed a more spectrum- and energy-efficient alternative to the standard CP-OFDM scheme, whereby the theory of SCS is exploited to enable TDS-OFDM to support high-order modulation schemes such as 256QAM in realistic static channels with large delay spread and HDTV delivery in fast fading channels. This is achieved by utilizing the sparsity and inter-channel correlation of wireless channels in a simultaneous multi-channel reconstruction procedure, whereby multiple IBI-free regions of very small size within consecutive TDS-OFDM symbols are used under the framework of SCS. In this way, not only an obviously improved channel reconstruction accuracy is achieved, but also the mutually conditional time-domain channel estimation and frequency-domain data detection in conventional TDS-OFDM can be decoupled without the use of iterative interference cancellation. Since the proposed scheme requires no modification of the basic signal structure of TDS-OFDM, a high spectrum efficiency is inherited, and furthermore the guard interval amplitude can be decreased to improve the energy efficiency. It is shown that the proposed scheme outperforms CP-OFDM in spectrum and energy efficiency by more than 10% and 20%, respectively. In addition, due to the similarity in signal structure, the methods proposed in this paper are directly applicable to other TS-aided transmission schemes like KSP-OFDM, PRP-OFDM, UW-OFDM, and UW-SC.

Acknowledgement

We would like to thank Prof. Feifei Gao from Tsinghua University for his valuable discussions and helpful suggestions to improve the quality of this paper.

References

[1] C. Han, T. Harrold, S. Armour, I. Krikidis, S. Videv, P. Grant, H. Haas, J. Thompson, I. Ku, C. Wang *et al.*, "Green radio: radio techniques to enable energy-efficient wireless networks," *IEEE Commun. Mag.*, vol. 49, no. 6, pp. 46–54, Jun. 2011.

[2] J. Ketonen, M. Juntti, and J. Cavallaro, "Performance-complexity comparison of receivers for a LTE MIMO–OFDM system," *IEEE Trans. Signal Process.*, vol. 58, no. 6, pp. 3360–3372, Jun. 2010.

[3] T. van Waterschoot, V. Le Nir, J. Duplicy, and M. Moonen, "Analytical expressions for the power spectral density of CP-OFDM and ZP-OFDM signals," *IEEE Signal Process. Lett.*, vol. 17, no. 4, pp. 371–374, Apr. 2010.

[4] L. Dai, Z. Wang, and Z. Yang, "Time-frequency training OFDM with high spectral efficiency and reliable performance in high speed environments," *IEEE J. Sel. Areas Commun.*, vol. 30, no. 4, pp. 695–707, May 2012.

[5] R. Martin, K. Vanbleu, M. Ding, G. Ysebaert, M. Milosevic, B. Evans, M. Moonen, and C. Johnson Jr, "Unification and evaluation of equalization structures and design algorithms for discrete multitone modulation systems," *IEEE Trans. Signal Process.*, vol. 53, no. 10, pp. 3880–3894, Oct. 2005.

[6] D. Van Welden and H. Steendam, "Near optimal iterative channel estimation for KSP-OFDM," *IEEE Trans. Signal Process.*, vol. 58, no. 9, pp. 4948–4954, Sep. 2010.

[7] *Error-correction, data framing, modulation and emission methods for digital terrestrial television broadcasting*. Recommendation ITU-R BT. 1306-6, Dec. 6, 2011.

[8] L. Dai, Z. Wang, and Z. Yang, "Next-generation digital television terrestrial broadcasting systems: Key technologies and research trends," *IEEE Commun. Mag.*, vol. 50, no. 6, pp. 150–158, Jun. 2012.

[9] *Digital Video Broadcasting (DVB); Frame Structure, Channel Coding and Modulation for a Second Generation Digital Terrestrial Television Broadcasting System (DVB-T2)*. ETSI Standard, EN 302 755, V1.3.1, Apr. 2012.

[10] G. Hiertz, D. Denteneer, L. Stibor, Y. Zang, X. Costa, and B. Walke, "The IEEE 802.11 universe," *IEEE Commun. Mag.*, vol. 48, no. 1, pp. 62–70, Jun. 2010.

[11] J. Wang, Z. Yang, C. Pan, and J. Song, "Iterative padding subtraction of the PN sequence for the TDS-OFDM over broadcast channels," *IEEE Trans. Consum. Electron.*, vol. 51, no. 11, pp. 1148–1152, Nov. 2005.

[12] S. Tang, K. Peng, K. Gong, J. Song, C. Pan, and Z. Yang, "Novel decision-aided channel estimation for TDS-OFDM systems," in *Proc. IEEE International Conference on Communications (ICC'08)*, May 2008, pp. 946–950.

[13] J. Lin, "Channel estimation assisted by postfixed pseudo-noise sequences padded with zero samples for mobile orthogonal-frequency-division-multiplexing communications," *IET Commun.*, vol. 3, no. 4, pp. 561–570, Apr. 2009.

[14] M. Liu, M. Crussiere, and J.-F. Helard, "A combined time and frequency algorithm for improved channel estimation in TDS-OFDM," in *IEEE International Conference on Communications (ICC'10)*, May 2010, pp. 1–6.

[15] D. H. Sayed, M. Elsabrouty, and A. F. Shalash, "Improved synchronization, channel estimation, and simplified LDPC decoding for the physical layer of the DVB-T2 receiver," *EURASIP J. Wireless Communi. Net.*, vol. 2013, no. 1, pp. 1–16.

[16] M. Liu, M. Crussiere, and J.-F. Helard, "A novel data-aided channel estimation with reduced complexity for TDS-OFDM systems," *IEEE Trans. Broadcast.*, vol. 58, no. 2, pp. 247–260, Jun. 2012.

[17] M. Huemer, C. Hofbauer, and J. B. Huber, "Non-systematic complex number RS coded OFDM by unique word prefix," *IEEE Trans. Signal Process.*, vol. 60, no. 1, pp. 6073–6085, Jan. 2012.

[18] L. Dai, J. Fu, J. Wang, and J. Song, "A multi-user uplink TDS-OFDM system based on dual PN sequence padding," *IEEE Trans. Consum. Electron.*, vol. 55, no. 3, pp. 1098–1106, Aug. 2009.

[19] J. Fu, J. Wang, J. Song, C. Pan, and Z. Yang, "A simplified equalization method for dual PN-sequence padding TDS-OFDM systems," *IEEE Trans. Broadcast.*, vol. 54, no. 4, pp. 825–830, Dec. 2008.

[20] L. Dai, Z. Wang, and Z. Yang, "Spectrally efficient time-frequency training OFDM for mobile large-scale MIMO systems," *IEEE J. Sel. Areas Commun.*, vol. 31, no. 2, pp. 251–263, Feb. 2013.

[21] D. Donoho, "Compressed sensing," *IEEE Trans. Inf. Theory*, vol. 52, no. 4, pp. 1289–1306, 2006.

[22] J. A. Tropp, A. C. Gilbert, and M. J. Strauss, "Algorithms for simultaneous sparse approximation. part i: Greedy pursuit," *Signal Processing*, vol. 86, no. 3, pp. 572–588, 2006.

[23] L. Dai, Z. Wang, and S. Chen, "A novel uplink multiple access scheme based on TDS-FDMA," *IEEE Trans. Wireless Commun.*, vol. 10, no. 3, pp. 757–761, Mar. 2011.

[24] B. Yang, K. Letaief, R. Cheng, and Z. Cao, "Channel estimation for OFDM transmission in multipath fading channels based on parametric channel modeling," *IEEE Trans. Commun.*, vol. 49, no. 3, pp. 467–479, Mar. 2001.

[25] W. Bajwa, J. Haupt, A. Sayeed, and R. Nowak, "Compressed channel sensing: A new approach to estimating sparse multipath channels," *Proc. IEEE*, vol. 98, no. 6, pp. 1058–1076, Jun. 2010.

[26] C. Berger, Z. Wang, J. Huang, and S. Zhou, "Application of compressive sensing to sparse channel estimation," *IEEE Commun. Mag.*, vol. 48, no. 11, pp. 164–174, Nov. 2010.

[27] I. Telatar and D. Tse, "Capacity and mutual information of wideband multipath fading channels," *IEEE Trans. Inf. Theory*, vol. 46, no. 4, pp. 1384–1400, Jul. 2000.

[28] S. Borade and L. Zheng, "Writing on fading paper, dirty tape with little ink: Wideband limits for causal transmitter CSI," *IEEE Trans. Inf. Theory*, vol. 58, no. 8, pp. 5388–5397, Aug. 2012.
[29] *Guideline for Evaluation of Radio Transmission Technology for IMT-2000*. Recommendation ITU-R M. 1225, 1997.
[30] E. Van Den Berg and M. Friedlander, "Theoretical and empirical results for recovery from multiple measurements," *IEEE Trans. Inf. Theory*, vol. 56, no. 5, pp. 2516–2527, May 2010.
[31] M. Duarte and Y. Eldar, "Structured compressed sensing: from theory to applications," *IEEE Trans. Signal Process.*, vol. 59, no. 9, pp. 4053–4085, Sep. 2011.
[32] F. Wan, W. Zhu, and M. Swamy, "Semi-blind most significant tap detection for sparse channel estimation of OFDM systems," *IEEE Trans. Circuits Syst. I, Reg. Papers*, vol. 57, no. 3, pp. 703–713, Mar. 2010.
[33] S. M. Kay, *Fundamentals of Statistical Signal Processing, Volumn I: Estimation Theory*. New Jersey, USA: Prentice-Hall, 1993.
[34] M. Varanasi, C. Mullis, and A. Kapur, "On the limitation of linear MMSE detection," *IEEE Trans. Inf. Theory*, vol. 52, no. 9, pp. 4282–4286, Sep. 2006.
[35] J. Haupt, W. Bajwa, G. Raz, and R. Nowak, "Toeplitz compressed sensing matrices with applications to sparse channel estimation," *IEEE Trans. Inf. Theory*, vol. 56, no. 11, pp. 5862–5875, Nov. 2010.
[36] F. Yang, J. Wang, and Z. Yang, "Novel channel estimation method based on PN sequence reconstruction for Chinese DTTB system," *IEEE Trans. Consum. Electron.*, vol. 54, no. 4, pp. 1583–1588, Nov. 2008.
[37] R. V. Nee and R. Prasad, *OFDM for wireless multimedia communications*. Chichester, UK: Artech House, Inc., 2000.

Linglong Dai (M'11) received his B.S. degree from Zhejiang University in 2003, the M.S. degree (with the highest honor) from the China Academy of Telecommunications Technology (CATT) in 2006, and the Ph.D. degree (with the highest honor) from Tsinghua University in 2011. From 2011 to 2013, he was a Postdoctoral Fellow at the Department of Electronic Engineering, Tsinghua University. From July 2013, he is an Assistant Professor with the Department of Electronic Engineering, Tsinghua University, Beijing, China. His research interests are in wireless communications with the emphasis on OFDM, MIMO, synchronization, channel estimation, multiple access techniques, and wireless positioning. He has published over 30 journal and conference papers. He has received IEEE ICC Best Paper Award in 2013, Outstanding Postdoctoral Fellow of Tsinghua University in 2013, China Postdoctoral Science Special Foundation in 2012, Excellent Doctoral Dissertation of Beijing in 2012, Outstanding Ph.D. Graduate of Tsinghua University in 2011, and Academic Star of Tsinghua University in 2011.

Jintao Wang (M'06-SM'11) received his B.Eng and Ph.D degrees in Electrical Engineering both from Tsinghua University, Beijing, China in 2001 and 2006, respectively. From 2006 to 2009, he was an assistant professor in the Department of Electronic Engineering at Tsinghua University. Since 2009, he has been an associate professor and Ph.D supervisor. He is the standard committee member for the Chinese national digital terrestrial television broadcasting standard. His current research interests include space-time coding, MIMO and OFDM systems. Dr. Wang has published more than 40 journal and conference papers and holds 18 National Invention Patents.

Zhaocheng Wang (M'09-SM'11) received his B.S., M.S. and Ph.D. degrees from Tsinghua University in 1991, 1993 and 1996, respectively. From 1996 to 1997, he was with Nanyang Technological University (NTU) in Singapore as a Post Doctoral Fellow. From 1997 to 1999, he was with OKI Techno Centre (Singapore) Pte. Ltd., firstly as a research engineer and then as a senior engineer. From 1999 to 2009, he worked at SONY Deutschland GmbH, firstly as a senior engineer and then as a principal engineer. He is currently a Professor at the Department of Electronic Engineering, Tsinghua University. His research areas include wireless communications, digital broadcasting and millimeter wave communications. He holds 29 granted US/EU patents and has published over 70 technical papers. He has served as technical program committee co-chair/member of many international conferences. He is a Senior Member of IEEE and a Fellow of IET.

Paschalis Tsiaflakis (S'06-M'09) received the M.Eng. degree in information and communication technology from the Katholieke Hogeschool Limburg (Belgium) in 2001, and the M.S. degree and Ph.D. degree, both in electrical engineering, from the KU Leuven (Belgium) in 2004 and 2009, respectively.

He is currently an FWO Postdoctoral Research Fellow with the Department of Electrical Engineering, KU Leuven. Since 2004, he has been involved in several industrial research projects in cooperation with Alcatel-Lucent, Belgium. He was a visiting scholar at Princeton University in 2007, a visiting postdoc at the University of California Los Angeles in 2010, and a postdoctoral fellow in the Center for Operations Research and Econometrics at UCL (Belgium) in 2011. His research interests include signal processing and optimization for digital communication systems.

Dr. Tsiaflakis received the 'Belgian Young ICT Personality 2010 Award' in 2010, the 'Best Multimedia Master Thesis Prize' in 2001, and was a top-12 finalist for the European ERCIM Cor Baayen Award in 2010. He also received an FWO Aspirant scholarship (2004-2008), an FWO grant for a visiting research collaboration at Princeton University in 2007, a PDMK postdoc grant in 2009, an ASL grant for a research visit at UCLA in 2010, a Francqui Intercommunity Postdoc Grant in 2011, and an FWO postdoc grant (2011-2014).

Marc Moonen (M'94-SM'06-F'07) received the electrical engineering degree and the PhD degree in applied sciences from KU Leuven, Belgium, in 1986 and 1990 respectively. Since 2004 he is a Full Professor at the Electrical Engineering Department of KU Leuven, where he is heading a research team working in the area of numerical algorithms and signal processing for digital communications, wireless communications, DSL and audio signal processing. He received the 1994 K.U.Leuven Research Council Award, the 1997 Alcatel Bell (Belgium) Award (with Piet Vandaele), the 2004 Alcatel Bell (Belgium) Award (with Raphael Cendrillon), and was a 1997 Laureate of the Belgium Royal Academy of Science. He received a journal best paper award from the IEEE Transactions on Signal Processing (with Geert Leus) and from Elsevier Signal Processing (with Simon Doclo). He was chairman of the IEEE Benelux Signal Processing Chapter (1998-2002), and a member of the IEEE Signal Processing Society Technical Committee on Signal Processing for Communications, and is currently President of EURASIP (European Association for Signal Processing).

He has served as Editor-in-Chief for the *EURASIP Journal on Applied Signal Processing* (2003-2005), and has been a member of the editorial board of *IEEE Transactions on Circuits and Systems II*, *IEEE Signal Processing Magazine, Integration, The VLSI Journal*, *EURASIP Journal on Wireless Communications and Networking, and Signal Processing*. He is currently a member of the editorial board of EURASIP Journal on Applied Signal Processing and Area Editor for Feature Articles in the *IEEE Signal Processing Magazine*.